Acta of Bioengineering and Biomechanics

# Encrustation of the Ureteral Double-J Stents Made of Styrene/Ethylene/Butylene and Polyurethane Before and After Implantation

**Keywords**

Young's modulus, SEM observation, stone disease, urologic surgical procedure, DJ catheter, encrustation

**Abstract**

Purpose

The aim of this study was to determine the affinity to crystal, calculi, and biofilm deposition on ureteral double-J stents (DJ stents) after ureterorenoscopic–lithotripsy procedure (URS-L). The analysis was performed in two aspects: to determine which materials used for fabricating ureteral stents promotes encrustation and which part of the DJ stents is the most vulnerable for blockage.

Methods

One hundred twenty patients with an indwelling DJ stent duration between 7 and 78 days were included in this study. The encrustation of DJ stents was characterized by scanning electron microscopy (SEM), and the mechanical properties of DJ stents were examined using the standard MTS Micro Bionix tensile test.

Results

This study showed that polyurethane catheters have a much higher affinity for encrustation than styrene/ethylene/butylene block copolymer. Obtained results indicated the proximal (renal pelvis) and distal (urinary bladder) part is the most susceptible to post-URS-L fragments and urea salt deposition. Both the DJ ureteral stents' outer and inner surfaces were completely covered even after 7 days of implantation.

Conclusions

Performed analysis pointed out that polyurethane DJ stents have a much higher affinity for encrustation of calculi and NaCl crystals compared to the silicone-based copolymer. The surface of the ureteral stents needs improvement to minimize salt and kidney stone deposition, causing pre-biofilm formation and the occurrence of defects and cracks.

**Authors**

Dr. Adam Haliński
Department of Clinical Genetics and Pathology, University of Zielona Gora, Licealna 9 Street, 65-417 Zielona Gora, Poland;

Scientific Office, U-merge Ltd., London-Athens-Dubai, Menandrou Street Athens 14561, Greece;

Kamila Pasik
Department of Biomedical Engineering, University of Zielona Gora, Licealna 9 Street, 65-417 Zielona Gora, Poland;

Andrzej Haliński
Department of Paediatric Urology, "Klinika Wisniowa", "Cherry Clinic", Anieli Krzywon 2 Street, 65-534 Zielona Gora, Poland;

Paweł Haliński
Department of Paediatric Urology, "Klinika Wisniowa", "Cherry Clinic", Anieli Krzywon 2 Street, 65-534 Zielona Gora, Poland;

Alberto Trinchieri

Scientific Office, U-merge Ltd., London-Athens-Dubai,
Menandrou Street Athens 14561, Greece;

Noor Buchholz
Scientific Office, U-merge Ltd., London-Athens-Dubai,
Menandrou Street Athens 14561, Greece;

**Prof. Katarzyna Arkusz**
Department of Biomedical Engineering, University of Zielona
Gora, Licealna 9 Street, 65-417 Zielona Gora, Poland;

**Explanation letter**

EXPLANATION LETTER - attached file

Explanation letter.pdf

## 1. Introduction

A common chronic kidney condition that pertains to urological patients is urolithiasis, leading to urinary stones. The mentioned problem is a common problem with a worldwide estimated 20% prevalence, which will grow significantly over the coming years [11]. This is estimated to a 5-year recurrence rate of 50%, and the incidence and prevalence of kidney stones are increasing globally [2]. Ureteral obstruction is caused by kidney stones disorder, renal function, and intensifies patient pain [35].

A double-J ureteral stent implantation is a common surgical procedure aiming at ureteral drainage to assure renal function, treat pain caused by ureteral obstruction, and avoid external or visible devices [20]. The most common materials used as ureteral stents are polyethylene, polyurethane, and silicone [15], [32]. The type of material affects the patient's body response, hence the required characteristics such as biocompatible, antimicrobial, and antifouling [28]. Furthermore, materials required for urinal catheterization are defined by their mechanical properties: low surface roughness [18], high mechanical strength, and flexibility [28]. Among these materials, silicone stents may be more advantageous than polyurethane stents due to the lower risk of calcification and prolonged maintenance of tensile strength for up to 20 months [1]. However, no comparable research has been performed yet.

Ureteric stents have been deployed for over four decades, and as their technique is upgrading, their complications have expanded (e.g., stent migration, encrustation, stone formation, and fragmentation) [1]. Short-term stenting for stone removal (<6 weeks) represents an immense economic burden. When in contact with urine, ureteral stents frequently become covered by calcium phosphate and calcium oxalate crystal-containing encrustations, which can damage the uroepithelium and pain and have been proposed to promote infections [25, 8]. Hitherto, studies of ureteral stenting included determination of effective urine flow from the kidney to the bladder [13] – [14], structural and chemical composition investigation [9], [32], [33], and shape and size optimization [24], [31]. The urine flow consists of in-stent (luminal) and out-of-stent (extraluminal) flows, whereas lower flow rates were observed with larger DJ stents [13] and increasing the number of side holes increased the overall flow rate [14]. Encrustation and pain increase with the diameter of the indwelling ureter stent [24]. It is important to note that encrustation is a serious complication of ureteral stent use, affecting the removal procedure. The encrustation of ureteral stents may be due to the deposition of organic layers (conditioning film), uropathogens, and salts in the urine. Encrustation at the distal end is less than the proximal one and calcium content, which is lower in the distal coil [33]. On the other hand, there can be differences in encrustation composition at each end of a stent [30],

[32]. Additionally, the deposition of calculi or crystal promoted biofilm formation, affecting the urinary tract infection [27].

This paper focuses on determining which materials among those commonly used in ureteral stents show the greatest affinity for biofilm formation and which part of the DJ stent is the most vulnerable to kidney stone formation in time. Therefore, there is a need to study the mechanism of formation of kidney stones on the ureteral stent's surface and methods to prevent these processes and study the influence of these structures on the mechanical properties of a ureteral stent.

## 2. Materials and Methods

### *2.1. Materials*

In total, 120 double-J ureteral stents (DJ stents) were removed from renal stone patients and recruited to the study between January 2019 and May 2021. All ureteral stents were obtained from patients who had been diagnosed with calcium oxalate urolithiasis.

Firstly, the most susceptible material for biofilm formation was indicated. DJ stents of two manufacturers were examined 31 days after their initial ureteral placement in adult patients after the ureterorenoscopic – lithotripsy (URS-L) to treat calcium oxalate stone. The first kind of DJ stents was built with a proprietary silicone-modified styrene/ethylene/butylene block copolymer (copolymer DJ stents); the second was a classic polyurethane stent. The polyurethane DJ stent accounted for 25% of all analyzed samples (30 pcs).

Secondly, the influence of implantation time to encrustation and biofilm formation was examined. The copolymer DJ stents after the URS-L, which implantation period lasted from 7 to 78 days, were examined using scanning electron microscopy. Each of the polyurethane stents were implanted for 31 days (25%, 30 pcs.), while the copolymer DJ stents were implanted for 7 days (8.3%, 10 pcs.), 17 days (11.7%, 14 pcs.), 25 days (8.3%, 10 pcs.), 31 days (35.9%, 43 pcs.) and 78 days (10.8%, 13 pcs.).

### *2.2. Surface analysis of stents*

A microscopic analysis was performed on the ureteral stents implanted after the URS-L. The microscopic observation was performed by the scanning electron field emission microscope JEOL JSM 7600F ~~equipped with an X-ray analyzer INCA OXFORD~~ (SEM). The microscopic analysis of the ureteral stents required an additional sample preparation procedure [3], [25]. The ureteral stent surface was sputtered with a chromium layer with a thickness of 5 nm. Representative polyurethane and copolymer DJ stents before and after implantation for 31 days were characterized by Fourier transform infrared spectroscopy (FTIR) (Thermo Scientific™ Nicolet™ iS50 FTIR Spectrometer, Thermo Scientific™, USA). Data were collected in the

absorption mode between 4000 $cm^{-1}$ and 400 $cm^{-1}$ with a resolution of 4 $cm^{-1}$. Room temperature and humidity during all process were maintained stable at 23˚C and 35%, respectively.

*2.3. Mechanical testing of DJ stents*

Tensile strength and stiffness were tested for all DJ stents before and after urinary exposure. The tensile strength was measured using an MTS Micro Bionix Testing System with Testworks II software, using a 5 N load cell. DJ stents were tested in uniaxial tension at 1 mm/s for 1 second. A preconditioning run was done for each stent, including a 3-minute hold time at 5 mm with 30 seconds between the preconditioning run and the first trial. Each DJ stent was examined using the tensile test minimum times, keeping the same manner of reposition. Unpaired Student's t-test was used for the comparison of the two groups of implantation time for each DJ-stent. A value of $p < 0.05$ was considered statistically significant.

## 3. Results

*3.1. Influence of DJ stent composition on encrustation and fracture*

In the beginning, it should be noticed that each of the analyzed DJ stents (120 pct) was divided according to the stent material, implantation time. Each group was managed to the KUB (Kidney, Ureter, Bladder) encrusted ureteral stent scoring system, while the standard deviation in each group does not exceed 1. Then, each DJ stent was divided into three parts (proximal, middle, distal), and the database of SEM pictures of each section was analyzed to choose the most similar and repeated photos, which are presented in this section.

The surface morphologies of DJ stents, made of copolymer and polyurethane, implanted for 31 days in the patient's body, have been investigated using scanning electron microscopy, which is shown in Fig. 1. The proximal part of the DJ stents means "pigtail", placed in the renal pelvis, while the distal coil is placed in the urinary bladder. As shown in Fig. 1, the copolymer DJ stents are covered with a much smaller number of crystals than the polyurethane version. The distal and proximal part of the polyurethane DJ stent is covered with the most complex film presenting a multi-layered structure.

**Figure 1.** SEM images of a DJ stent made of styrene/ ethylene/ butylene block copolymer, and polyurethane, implanted for 31 days

Figure 2 presents the data for a representative DJ stent made of styrene/ ethylene/ butylene block copolymer, and polyurethane, before and after implantation for 31 days by FTIR.

Before the implantation, several IR characteristic peaks were observed for copolymer and polyurethane DJ stents (Figures 2A and B, respectively). Observed for copolymer DJ stent, the broad peaks around 2949 and 2917 $cm^{-1}$ corresponding to the C–H stretching from the alkyl groups. In the range, 1500-800 $cm^{-1}$, peaks at 1453 $cm^{-1}$ (C–H bending), 1260 $cm^{-1}$ (C–O

stretching), 1100 $cm^{-1}$ – 1000 $cm^{-1}$ (C–O stretching in C–O–H groups and COC groups), and 805 $cm^{-1}$ (C-H rocking mode) were observed.

After implantation of copolymer DJ stents for 31 days, new peaks appeared around 3300 $cm^{-1}$ was due to the hydrogen-bonded OH stretching vibrations, 1729 $cm^{-1}$ (carbonyl groups), 1697 $cm^{-1}$ (the C=O stretching), and 1597 $cm^{-1}$ (N-H plane stretch), the peak 1104 $cm^{-1}$ (phosphates).

Before the implantation, the IR spectrum for polyurethane DJ stents showed characteristic peaks at 3331 $cm^{-1}$ (stretching of the NH bond), 2948 and 2868 $cm^{-1}$ (alkane -CH stretching vibration), 1727 $cm^{-1}$ – 1700 $cm^{-1}$ (carbonyl absorption band), 1596 $cm^{-1}$ – 1527 $cm^{-1}$ (a shoulder) 1220 $cm^{-1}$ (C–O stretching of the carbonate group), 1174 $cm^{-1}$ (C-N and C-O stretching vibrations), 1111 $cm^{-1}$ and 1065 $cm^{-1}$ (ester C-O-C symmetric stretching vibration). After implantation for 31 days the new peaks occur at 2919 $cm^{-1}$ ($NH_4^+$ stretching), 1623 $cm^{-1}$ (the C=O stretching), 1452 $cm^{-1}$ (P=O stretching), 1375 $cm^{-1}$ (C-N stretching), 803 $cm^{-1}$ (C-C stretching), 526 $cm^{-1}$ (O-C-O bending).

**Figure 2.** SEM images of a DJ stent made of styrene/ ethylene/ butylene block copolymer, and polyurethane, implanted for 31 days

The mechanical properties of unused DJ stents and stents retrieved from patients following insertion from 7 to 31 days are presented in Fig. 3. The Young's modulus (E) was calculated for each DJ stent using engineering stress, which assumes no cross-sectional area changes. The DJ stent's mechanical strength made of polyurethane (E=628±21 kPa) was twice lower compared to copolymer one (E=1547±129 kPa). After implantation, the copolymer DJ stent was the stiffest and the DJ stent implanted for 31 days was characterized by the lowest stiffness (E=1065±90 kPa). Implantation caused the significant loss of mechanical strength of polyurethane DJ stents to a value of 325±10 kPa. There was no significant change in the ultimate force of ureteral stents following implantation during 25 days in comparison to 31 days for copolymer DJ stents.

~~An EDS study, presented in Fig. 2 are the average values measured from all analyzed copolymer DJ stents with standard deviation. According to the similar results obtained in each part of the copolymer DJ stent (proximal, middle, distal) we decided to show the average results of each measurement (53 copolymer DJ stents implanted for 31 days x 3 part of each stent = 159 EDS measurements in total). SEM picture in the distal part of copolymer DJ stent was shown as an example of an analyzed area in EDS measurements. EDS analysis confirmed the presence of carbon, oxygen, phosphorous and calcium in the layer covering the copolymer DJ stents removed from the patient's body after 31 days.~~

**Figure 3.** The results of tensile tests (Young's modulus and the breaking force) of DJ ureteral stent made of copolymer and polyurethane, implanted for 0-31 days, *$p < 0.05$, **$p < 0.005$, *** $p < 0.001$

*3.2. Mechanism of stone formation on DJ stent surface*

The outer and inner side of the copolymer DJ stents proximal parts, which were removed from the patients' bodies after 7, 17, and 78 days are shown in Fig. 4. The outer side of the proximal part of the DJ stents is covered over time – the thickness of this layer increased with the implantation period's increase. The most extensive agglomeration on the inner side was observed during the seventh day of implantation (Fig. 4B). The extension of implantation time leads to a continuous increase of the multilayer's thickness on the inner side of the proximal part of the DJ stents (Fig. 4D) until 17 days of implantation, and thereafter its further acceleration (Fig. 4F).

**Figure 4.** SEM images of a proximal part of DJ stents implanted for 7-78 days

The encrustation of the distal part of the DJ stents in varying time of implantation was shown in Fig. 5. During the first day of implantation, the outer (Fig. 5A) and inner (Fig. 5B) side of DJ stents were completely covered by the multilayer of calcium oxalate fragments. Extension of implantation time resulted in forming a compact layer, leading to pain and difficult removal. After 78-days implantation, the outer (Fig. 5E) and inner (Fig. 5F) side is completely covered by small calculus growing on one another.

**Figure 5.** SEM images of a distal part of DJ stents implanted for 7-78 days

## 4. Discussion

Prevention of stone-crystal-layer formation on DJ stents is essential due to increased pressure in the blocked stent, causing many clinical problems, such as vesicoureteral reflux, migration, encrustation, urinary infection, stent fracture, necrosis and ureteroarterial fistula [28], [35].

The first stage of research was to determine the influence of DJ stents composition on encrustation. As shown in Fig. 1, the distal and proximal part of the polyurethane DJ stent is covered with the most complex film presenting a multi-layered structure. This encrustation was classified as score 4 for polyurethane stents and as score 2 for copolymer stents on a scale for scoring encrustations on ureteral double-J stents elaborated by Roupret [30].

Further, the FTIR analysis (Fig. 2) was performed to characterize encrustations, especially identifying the calculi adsorbed components onto the DJ stent's surface. According to the literature, about 30 distinct components have been found in urinary calculi [36]. Thus, we

decided to compare the obtained IR spectrum only for the main component of urea and urinary calculi.

For copolymer DJ stent before implantation, as it can be seen in Fig. 2A, the main absorption peak in IR spectrum appeared in the wavenumber: 2429 $cm^{-1}$, 1453 $cm^{-1}$, 805 $cm^{-1}$ confirmed the styrene/ethylene/butylene structure, and the silicone covering by the presence of a peak in 2917 $cm^{-1}$, and 1100 $cm^{-1}$ – 1000 $cm^{-1}$. The FTIR spectra of the polyurethane DJ stents (Fig. 2B) confirmed the polyurethane structure with the typical carbonyl absorption band of the ester bond located at 1729 $cm^{-1}$, and a shoulder at 1697 $cm^{-1}$, which can be attributed to the urethane and urea carbonyl groups. The absorbance at 3300 $cm^{-1}$ is consistent with the stretching of the NH bond and is characteristic of the urethane and urea groups. The other characteristic bands are 2900 $cm^{-1}$ due to the alkane -CH stretching vibration, 1174 $cm^{-1}$ due to the coupled C-N and C-O stretching vibrations, and 1062 $cm^{-1}$ due to the ester C-O-C symmetric stretching vibration. As shown in Figures 2A and B, the peak intensity of the IR spectra changed significantly after the implantation of copolymer and polyurethane DJ stents. After the implantation of copolymer DJ stent for 31 days, the absorbed encrustation was identified mainly as calcium oxalate dihydrate (weddellite), characterized by four sharp peaks between wavenumbers 1600 $cm^{-1}$ – 777 $cm^{-1}$. Furthermore, the peak of 2918 $cm^{-1}$ (N-H stretching) indicated the presence of NH4+ (ammonium ion); therefore, the stone may be included in the type of ammonium ion calcium oxalate dihydrate, or the uric acid crystal may be absorbed onto the DJ surface. A peak that characterizes calcium oxalate kidney stone type was also found in the encrusted layer after 31 days of polyurethane DJ stents implantation.

Secondly, the influence of implantation time on mechanical degradation was briefly described in the literature comparing the tensile strength of varying types of DJ stents [12], [29]. To the best of our knowledge, only Gorman et al. performed an analysis of the influence of implantation time on the mechanical strength of DJ stents [10]. However, this research was carried out on polyethylene stents and in artificial fluid. In this paper, the preconditioning procedure relied on the results presented in the literature [21]. Subjecting the samples to cyclic loads that do not break them stabilizes their reactions before tested tension. Preconditioning helps to eliminate variable sample responses to a given load and achieve a steady state. The procedures applied to provide a reproducible mechanical response that is the basis of reliable results for analysis. Obtained results showed that increased implantation time caused a decrease in Young's modulus (Fig. 3), indicating that decreased stent rigidity had occurred. Loss of mechanical properties of polyurethane DJ stents results in lower ultimate force at its break. These observations clearly indicate higher stability and less degradation of copolymer DJ stents

implanted for 31 days. It also excludes the possibility of long-term use of polyurethane DJ stents. Moreover, the build-up of deposits on the stent surface causes increasing stiffness and greater susceptibility to cracks and fractures. These results are in accordance with several studies [7], [12], [25], [29]. Highly elastic and flexible materials are more likely to crack or bend in vivo, while more rigid materials could cause severe bladder urgency, hematuria, or fracture during long-term stenting [23], [34].

Additionally, the proximal and distal parts (Fig. 1) are more likely to be exposed to contact with the urea, which results in its element deposition. According to the lower encrustation of copolymer DJ stents, these stents were chosen to further research. The previous investigation on flow and encrustation of DJ stents pointed out that long-term stent use is associated with precipitation of salts from the urine and infection, leading to a build-up of crystalline deposits on the stent surface, resulting difficult and painful stent removing [8], [20], [28], [30], [32].

The obtained results showed that the DJ stents' inner and outer surfaces were covered and deposited with the crystals of urea and, more importantly, by the post-URS-L fragments. The outer and inner side of the proximal (Fig. 4) and distal (Fig. 5) parts of the copolymer DJ stents, which were removed from the patients' bodies after 7, 17, and 78 days were covered with a more complex, multilayer consisting mostly of precipitated crystals (NaCl) and post-URS-L fragments (calcium oxalate stone). Performed analysis showed that the encrustation at the distal end (Fig. 5) was less than the proximal one (Fig. 4) and calcium content, which was lower in the distal coil. This hypothesis is confirmed by the work of Sighinolf et al. [33] and Kim et al. [14], who suggests that the last side hole in the proximal coil of the stent, located in the renal pelvis and the first side hole of the shaft of the stent, located in the even side hole throughout the ureter is critical to a DJ stent to maximize its role in the upper urinary system. Similar observations were made with hemodialysis catheters in our previous research [15], [25]. The encrustation on the distal and proximal parts of copolymer DJ stents formed during the first 17 days after implantation was classified as score 6 on a scale for scoring encrustations [30]. Such a distribution of film components suggests that the ureteral stent's blockage is due to not only large kidney stones but also a continuous flow of small calculi growing on one another. The most extensive agglomeration was observed during the seventh day of implantation (Fig. 4B), which could be the result of cleaning the kidney of post-URS-L residues. This is a crucial moment in the blockage of the DJ stents. If the DJ stent diameter is too large, the flow rates are too low, extending the contact time of post-URS-L fragments with the surface of DJ stents, resulting in its blockage. If the diameter of the DJ stent has been chosen correctly, the extension of implantation time results in a continuous increase of the thickness of the multilayer on the

inner side of the proximal part of the DJ stents (Fig. 3D and 3F). Additionally, the calculi or crystal deposition promotes biofilm formation, which affects the urinary tract infection [13]. Performed results and previous research [6], [22] indicate the necessity to use antibacterial and anticoagulation coatings of DJ stents, such as nano-silver [4], metallic nanoparticles [26], nitrofurazone [19], chlorhexidine [37], polytetrafluoroethylene (PTFE), hydrogel [17], lysostaphin [16], and antibacterial and anticoagulation coatings [5].

## 5. Conclusions

Previous studies of DJ stents were performed to the material selection for biocompatibility and optimization of their shape to ensure free urine flow. The literature indicates the importance of side holes in the DJ stents and their impact on stents clogging, however, ignoring the impact of the material itself and implantation time.

This study showed that polyurethane DJ stents have a much higher affinity for encrustation of calculi compared to the silicone-based copolymer. Residues deposited on the surface form a homogeneous multi-layer, mainly composing of weddellite and uric acid crystal, which close the DJ stents' lumen and significantly affect the flow of urine. Further analysis showed that the most vulnerable segment is the proximal part of the DJ stent (the part located in the renal pelvis). Slightly fewer fragments of kidney stones and sodium crystals are deposited in distal section of the stents. Studies have shown that as soon as seven days after implantation, the DJ stents may be completely blocked if its diameter is not properly adjusted. It has been observed that the layer formed on the outer surface of the catheter increases with longer implantation time, which occurs faster than for the inner layer. Implantation results in loss of mechanical strength of polyurethane DJ stents after just 31 days, what explains the problem of cracking/damage of DJ stents in patients' body or in removing procedure.

The surface of the ureteral stents needs improvement to minimize salt and kidney stone deposition, causing pre-biofilm formation and the occurrence of defects and cracks.

## References

[1] AHALLAL Y., KHALLOUK A., JAMAL EL FASSI M., FARIH M.H., *Risk Factor Analysis and Management of Ureteral Double-J Stent Complications*, Rev Urol, 2011, 12(2-3), 147–151.

[2] AKRAM M., IDREES M., *Progress and prospects in the management of kidney stones and developments in phyto-therapeutic modalities*, Int J Immunopathol Pharmacol, 2019, 33, 1–5.

[3] ARKUSZ K., KRASICKA-CYDZIK E., *The effect of phosphates and fluorides, included in $TiO_2$ nanotubes layers on the performance of hydrogen*, Arch Metall Mater, 2018, 63(2), 1–8.

[4] ARKUSZ K., NYCZ M., PARADOWSKA E., PIJANOWSKA D.G., *Electrochemical stability of $TiO_2$ nanotubes deposited with silver and gold nanoparticles in aqueous environment*, Environ Nanotechnol Monit Manag, 2021, 15, 1–12.

[5] ARKUSZ K., PARADOWSKA E., NYCZ M., MAZUREK-POPCZYK J., BALDY-CHUDZIK K., *Evaluation of the Antibacterial Activity of Ag- and Au-Nanoparticles Loaded $TiO_2$ Nanotubes*, J Biomed Nanotech, 2020 16(9), 1416–1425.

[6] ARKUSZ K., PASIK K., HALINSKI A., HALINSKI A., *Surface analysis of ureteral stent before and after implantation in the bodies of child patients*, Urolithiasis 2020, 1–10.

[7] BARTKOWIAK-JOWSA M., BEDZINSKI R., SZARANIEC B., CHLOPAK J., *Mechanical, biological, and microstructural properties of biodegradable models of polymeric stents made of PLLA and alginate fibers*, Acta Bioeng Biomech, 2011, 13(4), 21–8.

[8] BUHMANN M.T., ABT D., NOLTE O., *Encrustations on ureteral stents from patients without urinary tract infection reveal distinct urotypes and a low bacterial load*, Microbiome, 2019, 7(60), 1–17.

[9] DAVENPORT K., KUMAR V., COLLINS J., MELOTTI R., TIMONEY A.G., KEELEY F.X., *New Ureteral Stent Design Does Not Improve Patient Quality of Life: A Randomized, Controlled Trial*, J Urol, 2011, 185(1), 175–178.

[10] GORMAN S.P., JONES D.S., BONNER M.C., AKAY M., KEANE P.F., *Mechanical performance of polyurethane ureteral stents in vitro and ex vivo*, Biomaterials, 1997, 18(20), 1379–1383.

[11] HALINSKI A., HALINSKI A.H., *Stone located in proximal part of the ureter - ESWL, URS-L, flexible URS, MicroPerc? Which approach should we choose in children-prospective study*, Eur Urol Suppl, 2017, 16(7), 2549.

[12] HENDLIN K., DOCKENDORF K., HORN C., PSHON N., LUND B., MONGA M., *Ureteral stents: Coil strength and durometer*, Urology, 2006, 68(1), 42–45.

[13] KIM K., KIM H., CHOI Y.H., LEE S.B., BABA Y., *Urine flow analysis using double J stents of various sizes in in vitro ureter models*, Int J Numer Method, 2020, 36(6), 1–12.

[14] KIM K.W., KIM H.H., CHOI Y.H., LEE S.B., BABA Y., SUH S.H., *Arrangement of side holes in a double J stent for high urine flow in a stented ureter*, J Mech Sci, 2020, 34(2), 949–954.

[15] KLOSKOWSKI T., JUNDZIŁ A., KOWALCZYK T., U*reter Regeneration–The Proper Scaffold Has to Be Defined*, PLoS One, 2014, 9(8), 1–13.

[16] KOTASKOVA I., OBRUCOVA H., MALISOVA B., VIDENSKA P., ZWINSOVA B., PEROUTKOVA T., FREIBERGER T., *Molecular techniques complement culture-based assessment of bacteria composition in mixed biofilms of urinary tract catheter-related samples*, Front Microbiol, 2019, 10, 462.

[17] KUROWIAK J., KACZMAREK-PAWELSKA A., MACKIEWICZ A.G., BEDZINSKI R. *Analysis of the Degradation Process of Alginate-Based Hydrogels in Artificial Urine for Use as a Bioresorbable Material in the Treatment of Urethral Injuries*, Processes, 2020, 8(3), 304.

[18] LAWRENCE E.L., TURNER I.G., *Materials for urinary catheters: a review of their history and development in the UK*, Med Eng Phys, 2005, 27(6), 443–453.

[19] LO J., LANGE D., CHEW B., *Ureteral stents and foley catheters-associated urinary tract infections: the role of coatings and materials in infection prevention*, Antibiotics, 2014, 3(1), 87–97.

[20] MILICEVIC S., BIJELIC R., JAKOVLJEVIC B., *Encrustation of the Ureteral Double J Stent in Patients with a Solitary Functional Kidney - a Case Report*, Med Arh., 2015, 69(4), 265–268.

[21] MILLER K. S., EDELSTEIN L., CONNIZZO B.K., SOSLOWSKY L.J. *Effect of Preconditioning and Stress Relaxation on Local Collagen Fiber Re-Alignment: Inhomogeneous Properties of Rat Supraspinatus Tendon*, J Biomech Eng, 2012, 134(3), 031007.

[22] MOSAYYEBI A., MANES C., CARUGO D., *Advances in Ureteral Stent Design and Materials*, Curr Urol Rep, 2018, 19(35), 1–9.

[23] MOSAYYEBI A., VIJAYAKUMAR A., YUE Q.Y., BRES-NIEWADA E., MANES C., CARUGO D., SOMANI B.K., *Engineering solutions to ureteral stents: material, coating and design*, Cent European J Urol, 2017, 70, 270–274.

[24] NESTLER S., WITTE B., SCHILCHEGGER L., JONES J., *Size does matter: ureteral stents with a smaller diameter show advantages regarding urinary symptoms, pain levels and general health*, World J Urol, 2019 38(4), 1059–106.

[25] NYCZ M., PARADOWSKA E., ARKUSZ K., KUDLINSKI B., KRASICKA-CYDZIK E., *Surface analysis of long-term hemodialysis catheters made of carbothane (poly(carbonate)urethane) before and after implantation in the patients' bodies*, Acta Bioeng Biomech, 2018, 20(2), 47–53.

[26] NYCZ M., PARADOWSKA E., ARKUSZ K., PIJANOWSKA D.G., *Influence of geometry and annealing temperature in argon atmosphere of $TiO_2$ nanotubes on their electrochemical properties*, Acta Bioeng Biomech, 2020, 22(1), 165–177.

[27] OZGUR B.C., EKICI M., YUCETURK C.N., BAYRAK O., *Bacterial colonization of double J stents and bacteriuria frequency*, Kaohsiung J Med Sci, 2013, 29(12), 658–661.

[28] PAWLIKOWSKI M., SKALSKI K., SOWINSKI T., *Hyper-elastic modelling of intervertebral disc polyurethane implant*, Acta Bioeng Biomech, 2013, 15(2), 1–8.

[29] PEDRO, R.N., HENDLIN, K., KRIEDBERG, C., MONGA, M., *Wire-Based Ureteral Stents: Impact on Tensile Strength and Compression*, Urology, 2007, 70(6), 1057–1059.

[30] ROUPRÊT M., DAUDON M., HUPERTAN V., GATTEGNO B., THIBAULT P., TRAXER O., *Can ureteral stent encrustation analysis predict urinary stone composition?*, Urology, 2005, 66(2), 246–251.

[31] SALI G.M., JOSHI H.B., *Ureteric stents: Overview of current clinical applications and economic implications*, Int J Urol, 2019, 27(1), 7–15.

[32] SCARNECIU I., BRATU O.G., COBELSCHI C.P., *The Risk Factors and Chemical Composition of Encrustation of Ureteral Double J Stents in Patients with Urolithiasis*, Rev. Chim., 2018, 69(12), 3406–3409.

[33] SIGHINOLFI M.C., SIGHINOLFI G.P., GALLI E., MICALI S., FERRARI N., MOFFERDIN A., BIANCHI G., *Chemical and Mineralogical Analysis of Ureteral Stent Encrustation and Associated Risk Factors*, Urology 2015, 86(4), 703–706.

[34] SINGHA P., LOCKLI J., HANDA H., *A review of the recent advances in antimicrobial coatings for urinary catheters*, Acta Biomater, 2017, 50, 20–40.

[35] WANG Y., ZHONG B., YANG X., WANG G., HOU P., MENG J., *Comparison of the efficacy and safety of URSL, RPLU, and MPCNL for treatment of large upper impacted ureteral stones: a randomized controlled trial*, BMC Urol., 2017, 17(1), 1–7.

[36] WARTY Y., HARYANTO, F., FITRI L., HAEKAL M., HERMAN H., *A Spatial Distribution Analysis on the Deposition Mechanism Complexity of the Organic Material of Kidney Stone*, J Biomed Phys Eng, 2020, 10(3), 273–282.

[37] ZELICHENKO G., STEINBERG D., LORBER G., FRIEDMAN M., ZAKS B., LAVY E., DUVDEVANI M., *Prevention of initial bioflm formation on ureteral stents using a sustained releasing varnish containing chlorhexidine. Vitro study*, J Endourol, 2013, 27(3), 333–337.

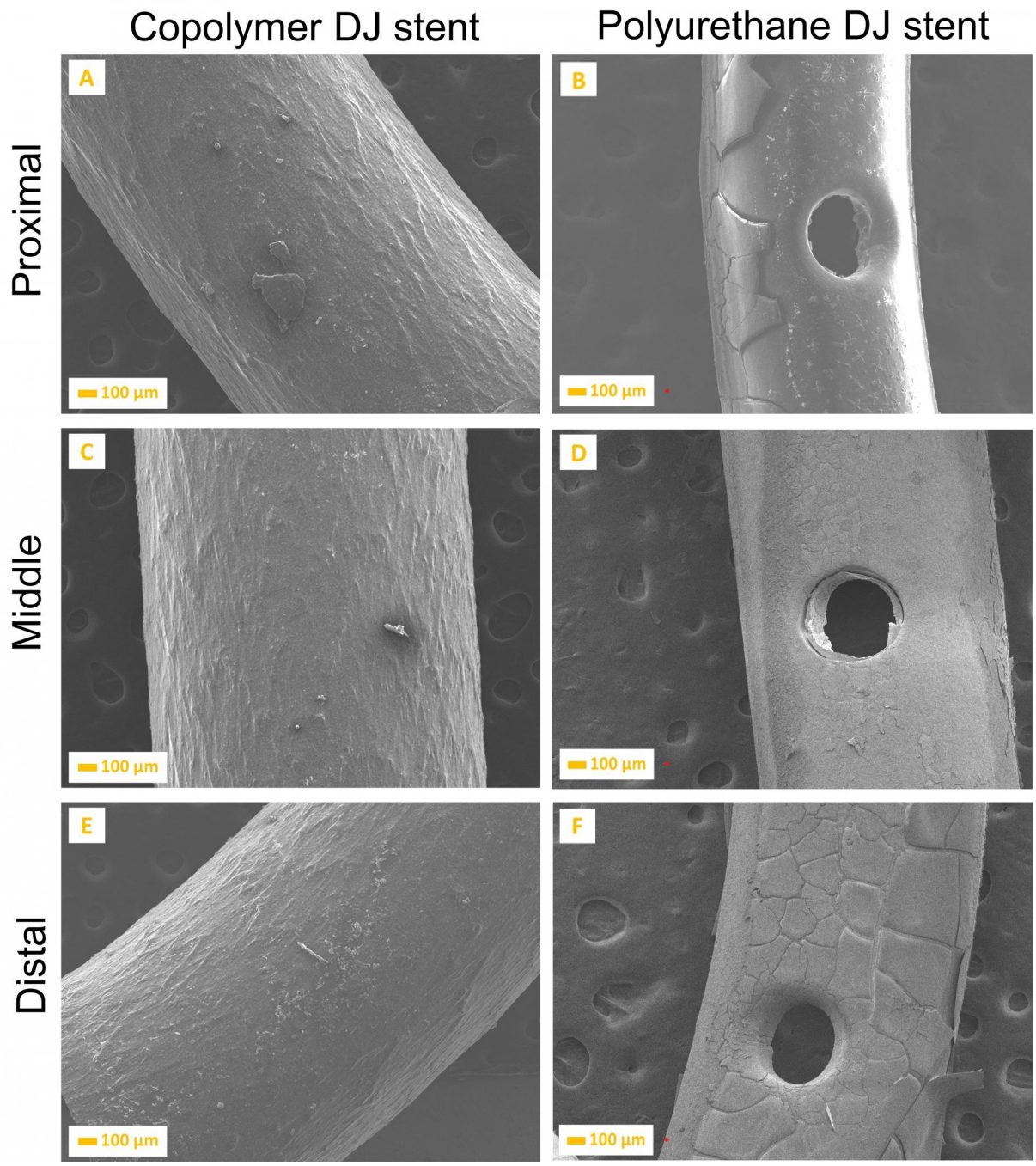


Figure 1. SEM images of a DJ stent made of styrene/ ethylene/ butylene block copolymer, and polyurethane, implanted for 31 days

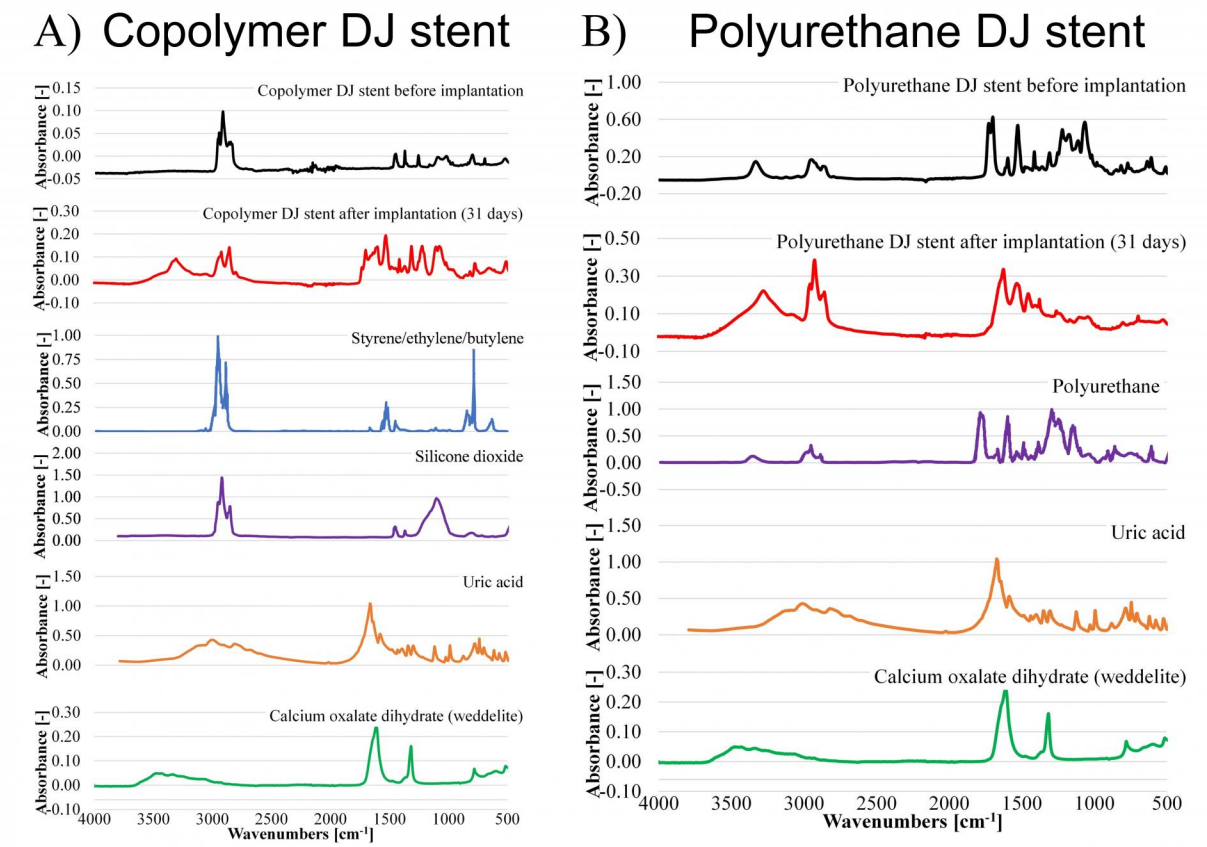


Figure 2. SEM images of a DJ stent made of styrene/ ethylene/ butylene block copolymer, and polyurethane, implanted for 31 days

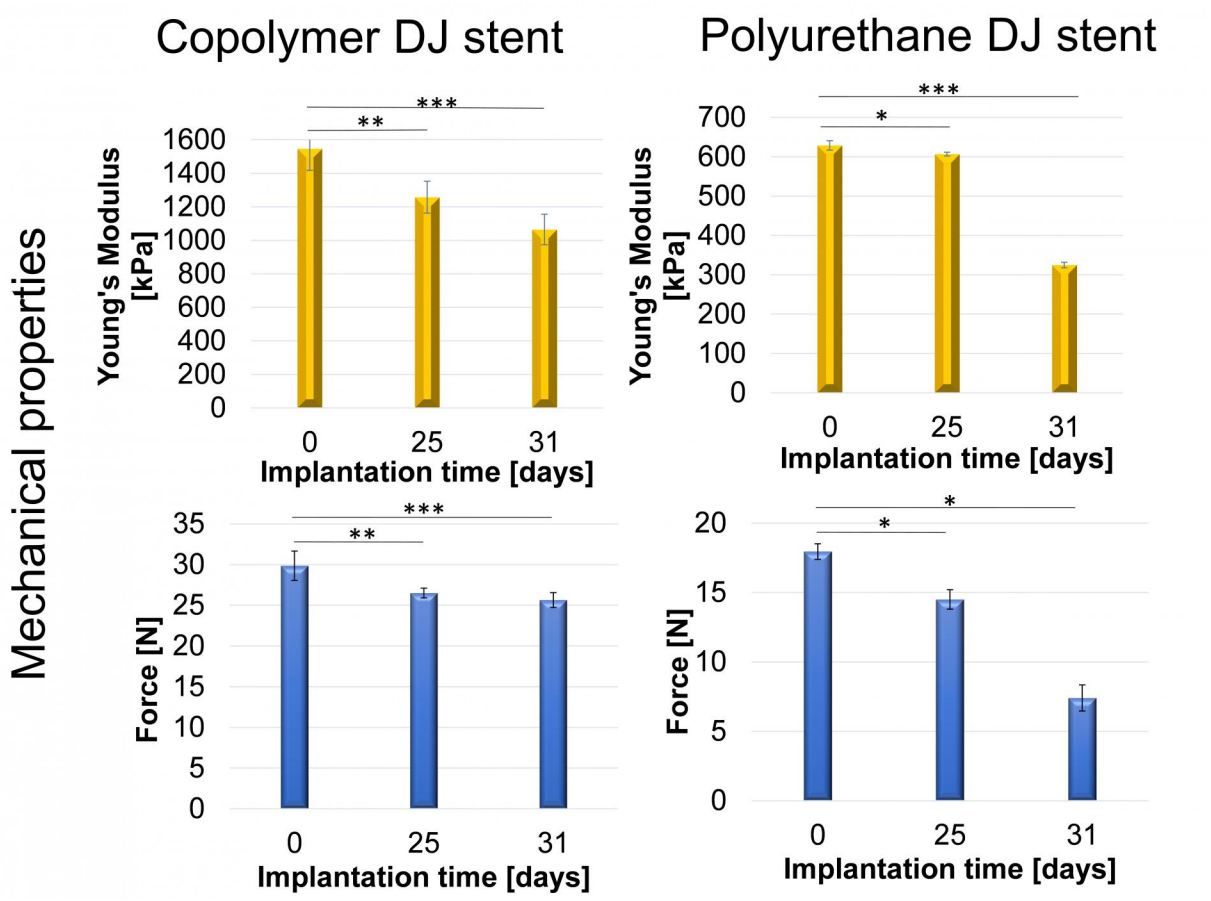


Figure 3. The results of tensile tests (Young's modulus and the breaking force) of DJ ureteral stent made of copolymer and polyurethane, implanted for 0-31 days, *p < 0.05, **p < 0.005, *** p < 0.001

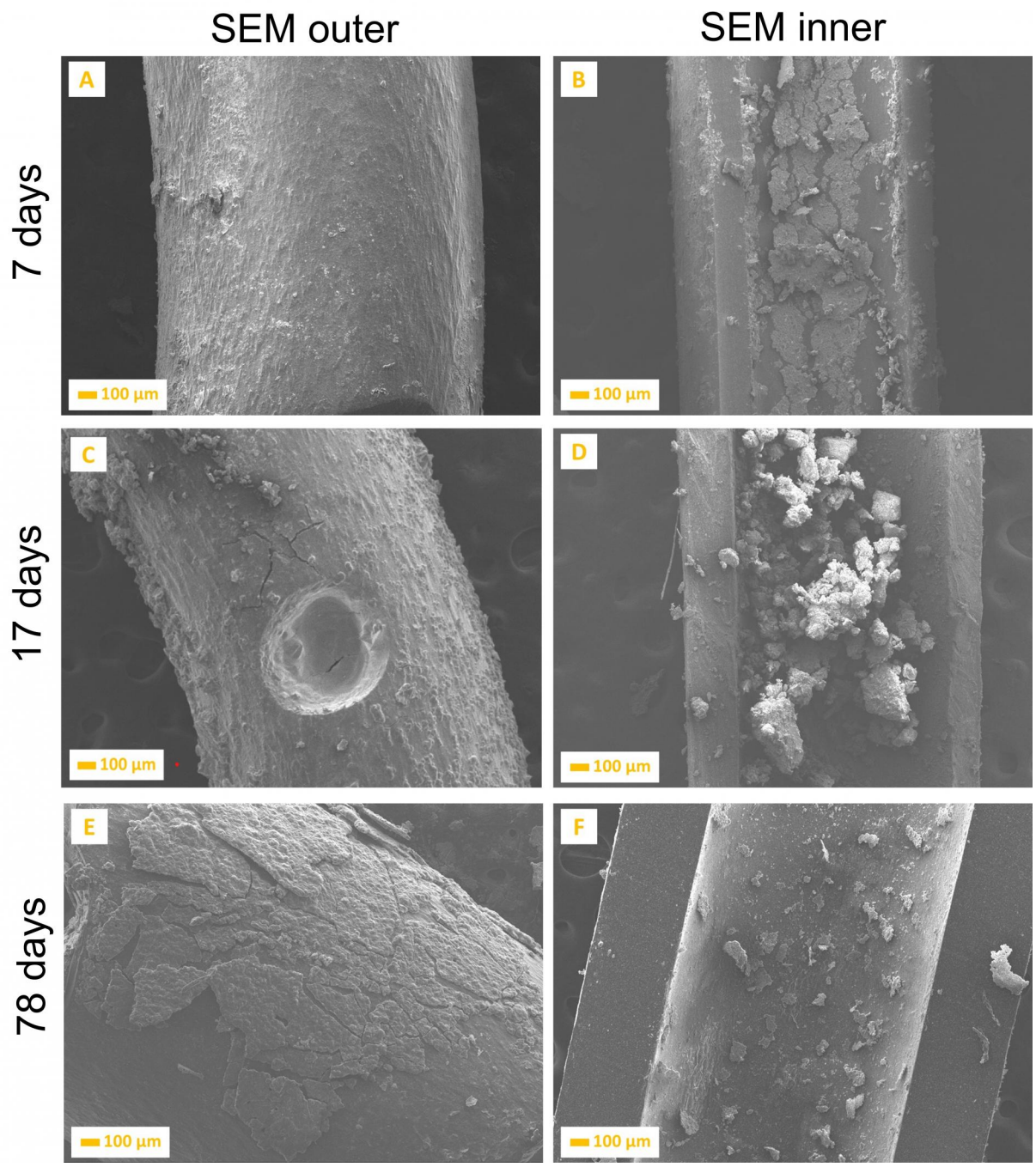


Figure 4. SEM images of a proximal part of DJ stents implanted for 7-78 days

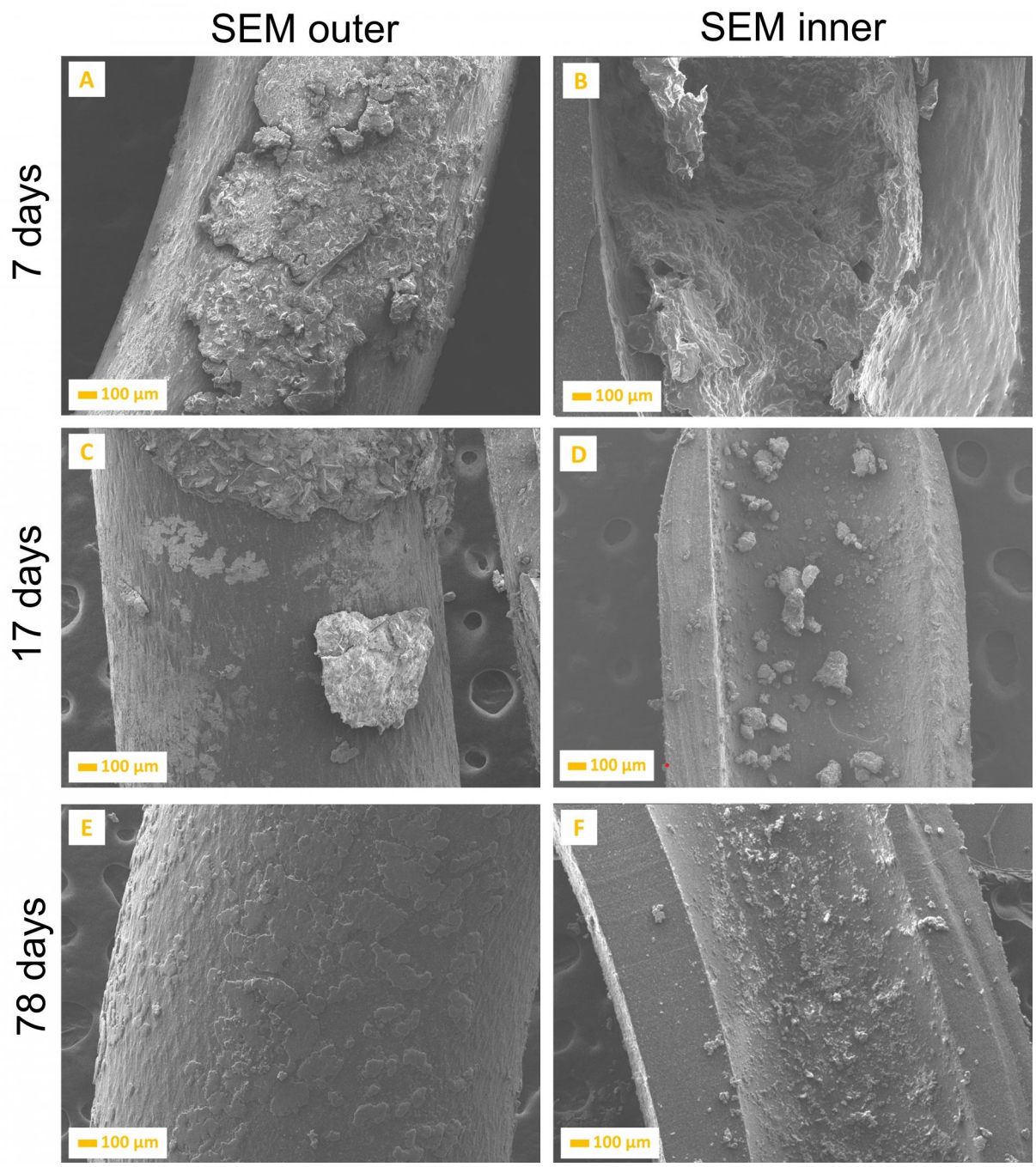


Figure 5. SEM images of a distal part of DJ stents implanted for 7-78 days

## Manuscript body

Download source file (37.68 kB)

## Figures

Figure 1 - Download source file (10.24 MB)
Figure 1. SEM images of a DJ stent made of styrene/ ethylene/ butylene block copolymer, and polyurethane, implanted for 31 days

Figure 2 - Download source file (4.76 MB)
Figure 2. SEM images of a DJ stent made of styrene/ ethylene/ butylene block copolymer, and polyurethane, implanted for 31 days

Figure 3 - Download source file (4.16 MB)
Figure 3. The results of tensile tests (Young's modulus and the breaking force) of DJ ureteral stent made of copolymer and polyurethane, implanted for 0-31 days, *$p < 0.05$, **$p < 0.005$, *** $p < 0.001$

Figure 4 - Download source file (8.25 MB)
Figure 4. SEM images of a proximal part of DJ stents implanted for 7-78 days

Figure 5 - Download source file (8.85 MB)
Figure 5. SEM images of a distal part of DJ stents implanted for 7-78 days